

# Validation of Hyperbolic Model by the Results of Triaxial and Direct Shear Tests of Municipal Solid Waste

Mohsen Asadi · Nader Shariatmadari · Mehran Karimpour-Fard · Ali Noorzad

Received: 22 November 2015 / Accepted: 22 March 2017 / Published online: 18 April 2017  
© Springer International Publishing Switzerland 2017

**Abstract** The increasing demand of engineering landfills requires that designers propose a framework for landfill design, construction, repair and maintenance. As municipal solid waste (MSW) is a major part of a landfill, the analysis should consider MSW mechanical behavior using a constitutive model. To investigate this, 18 direct shear (DS) and triaxial (TX) tests were conducted on MSW samples with different fiber contents. Different shearing mechanisms lead to understand effects of fibers on stress–strain response. Based on obtained results the hyperbolic model Duncan and Chang (J Soil Mech Found Div 96(5):1629–1653, 1970) has been employed to simulate the TX results indicating the ability of the model

to predict stress–strain behavior of MSW. This model could also be employed to the DS test results with some assumptions. The model can capture DS stress–strain response well whereas for TX tests the predictions were just enough. The experimental results and two sets of proposed MSW parameters of hyperbolic model have been compared and discussed.

**Keywords** Municipal solid waste · Hyperbolic model · Triaxial test · Direct shear test · Fiber content

## 1 Introduction

As the population increases and life style changes, the waste management tactics are also updated and governments try to find ways to reduce waste production and disposal. Lessening waste production needs making laws and public awareness. On the other hand, waste disposal can be reduced by recycling and reusing; however it's unavoidable and every city needs a disposal center.

Disastrous failures of landfills have been reported even in engineered ones resulting in people death and horrible environmental impacts (Blight 2008; Koerner and Soong 2000). Such reports show inadequate knowledge of landfill stability analysis.

Simulation and analysis of any structure, no difference how big it is, need at first understanding of mechanical behavior of its material and then based

---

M. Asadi (✉) · A. Noorzad  
Faculty of Civil, Water and Environmental Engineering,  
Shahid Beheshti University, East Vafadar Boulevard, 4th  
Tehranpars Square, Hakimieh,  
P.O. Box: 16765-1719, Tehran, Iran  
e-mail: mo\_asadi@sbu.ac.ir

A. Noorzad  
e-mail: a\_noorzad@sbu.ac.ir

N. Shariatmadari  
Department of Civil Engineering, Iran University of  
Science and Technology, 16846-13114 Narmak, Tehran,  
Iran  
e-mail: shariatmadari@iust.ac.ir

M. Karimpour-Fard  
Faculty of Engineering, The University of Guilan,  
41635-1477 Rasht, Iran  
e-mail: mehran.karimpour@guilan.ac.ir

on it adopting or developing a suitable model. These steps become challenging when modeling a landfill.

The mechanical behavior of Municipal Solid Waste, MSW, has been investigated widely in the last decades (e.g., Landva and Clark 1986; Grisolia et al. 1995; Machado et al. 2002; Vilar and Carvalho 2004; Bray et al. 2009; Shariatmadari et al. 2009; Babu et al. 2010; Zekkos et al. 2012; Karimpour-Fard et al. 2014). Because of high variety of the MSW composition, lack of a standard method of testing and no approved classification among scientists, reported results are significantly different. This suggests that particular studies are required for each site.

Even by reaching a consensus on MSW mechanical behavior, there are so many parameters affecting on it such as properties of waste components, waste composition, interaction of components, biodegradation, creep and etc. When modeling MSW, considering all of parameters, even if it was possible, makes the model impractical. With keeping in mind that modeling is to make a reality easier and simpler (Wood 2003), just the most effective parameters are taken into account and finding and understanding of them is important.

Besides constitutive models employed for soil modeling, a few models have been developed to indicate the MSW behavior exclusively, for example Machado et al. (2008) and Babu et al. (2010). Considering variability in composition, nonlinearity and inelasticity of waste, simulation of its behavior is a complex research field among other areas of the waste management.

Machado et al. (2002) introduced a constitutive model for MSW by considering waste as a material comprised of two major parts: organic paste and fiber. The authors employed the Cam-clay model for the paste fraction and the von Mises yield criterion for the fibers and then used them jointly to present the MSW behavior. This model considered effects of confining stress on fiber performance and mechanical creep on the response. The model was developed by Machado et al. (2008) to consider time dependent behavior of MSW. The influences of biodegradation of organic material and degradation of fibers on the mechanical behavior of MSW were considered in their new model. Model has remarkable capabilities such as considering stress path, mass loss of paste, variation of fiber properties during time and secondary creep; However model needs 21 variables which 8 of them represent

degradation process. The model can produce the typical stress–strain response of MSW, i.e. the primary downward curvature continuing with an upward concave at high levels of axial strain.

Babu et al. (2010) introduced a constitutive model for MSW behavior under loading according to the critical state framework. They adopted modified Cam-clay model with a change in volumetric strain calculation that was considering mechanical creep and time dependent biodegradation as well as elastic and plastic effects. Model needs eight parameters which four of them capture mechanical creep and biodegradation effects. To validate the model, they employed the results of small-scale triaxial tests on synthetic, fresh and degraded waste. Model predictions could capture linear response of MSW. Since in the model there is no consideration of fiber mobilization effects on MSW behavior, the ability of model to capture concavity at large strains is under question.

In this paper, the results of direct shear and triaxial tests conducted on MSW samples with different percentages of fibrous parts have been analyzed. Furthermore, the effect of fiber content on the mechanical response of MSW were investigated. Based on the results of each shearing apparatus, the hyperbolic model parameters are calculated and discussed. Hyperbolic model is a constitutive model employed for soil modeling and has been used to simulate MSW behavior (Reddy et al. 1996; Filz et al. 2001; Singh and Fleming 2010).

## 2 Materials and Methods

### 2.1 Sampling Procedure

The samples were collected from Kahrizak landfill in Tehran, Iran, located in the south of Kahrizak city. Kahrizak dumpsite started to accept Tehran's MSW since 1976 with an area of nearly 1400 acres. The daily input of MSW in this dumpsite is around 7000 tons mainly from Tehran and adjacent small counties.

Fresh samples were collected from the recycling site of Kahrizak dumpsite after removing large bulky and stiff parts and metals. Next, the samples (collected inside thick plastic bags) transferred to Geotechnical Research Center, GERC, in Iran University of Science & Technology, IUST. Figure 1 shows the composition

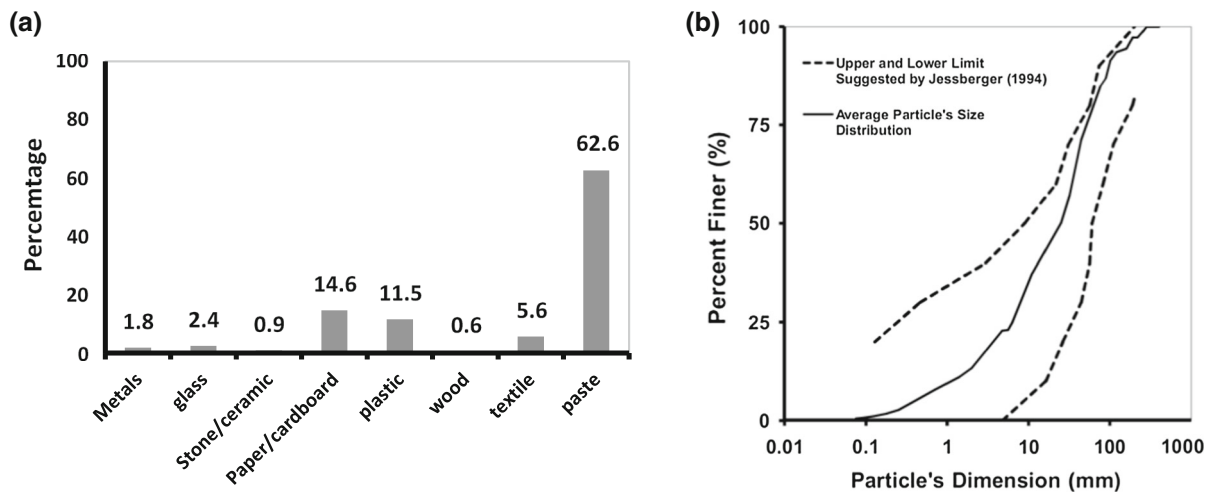


**Fig. 1** Fresh MSW of Kahrizak landfill: **a** composition (Shariatmadari et al. 2014), **b** average size distribution (Karimpour-Fard et al. 2014)

of fresh MSW and the grain size distribution curve of samples.

## 2.2 Sample Preparation

To prepare specimen for tests, all the sharp-tip objects, bulky rigid objects, plastic and vegetative fibers and all the fibrous parts and particles which could act as reinforcement materials were removed from the MSW.

Based on ASTM D4767-02 (2002), in triaxial tests, the maximum grain size of particles should be less than one-sixth of the sample's diameter. The diameter of samples in this research was 6 in. and as a result the maximum size of particles was limited to 1 in. (25 mm). The same upper limit was also employed in direct shear tests.

To address the effect of fiber content on the mechanical response of MSW, samples with different plastic contents of 0, 6 and 12% by weight were tested. To prepare these samples, as it was stated, first all the plastic fraction and foil-like materials inside the MSW were removed and then different percentages of new plastic fibers were added to the non-fibrous MSW.

A large-scale direct shear apparatus (box dimensions of 300 mm × 300 mm) and a large-scale triaxial apparatus (diameter of 150 mm) were used to examine the mechanical behavior of MSW samples.

Considering samples volume and proposed specific weight—that would be discussed in the following—,

for every test weights of fiber and paste fractions were determined and then they were mixed.

## 2.3 Test Parameters

Based on the in situ measurements of MSW density in Kahrizak dumpsite, an initial density of 9 kN/m<sup>3</sup> was used to prepare specimens. An upper limit of 100 kPa of normal stress was considered to conduct shear tests. Other normal stresses were 25 and 50 kPa.

Loading rate is an important factor in triaxial tests and could affect the results. Jessberger and Kockel (1993) and Carvalho (1999) employed a loading rate of 1 and 0.7 mm/min, respectively, and Karimpour-Fard et al. (2011) reported a loading rate of 0.8 mm/min for CD tests. In this research, the proper rate of loading was achieved by performing several tests. The criterion for this estimation was prevention of any excess pore pressure during the shearing stage. Based on these tests, a loading rate of 0.4 mm/min was chosen to perform triaxial and direct shear tests in consolidated drained (CD) condition.

In direct shear tests, the samples were compacted in three layers and saturated thereafter. After about 14 h, consolidation phase was started and lasted till negligible settlement of upper cap was observed; then shearing began. In triaxial tests, the samples were compacted inside the mold, mounted on pedestal, saturated using upward flow and back-pressure techniques, consolidated and finally sheared when rate of

**Table 1** Test schedule

Test ID	Fiber percentage	Normal (or confining) stress (kPa)	Initial unit weight (kN/m <sup>3</sup> )
DS-0-25	0	25	9.0
DS-0-50	0	50	9.0
DS-0-100	0	100	10.0
DS-6-25	6	25	9.0
DS-6-50	6	50	9.0
DS-6-100	6	100	9.2
DS-12-25	12	25	9.0
DS-12-50	12	50	9.0
DS-12-100	12	100	9.0
TX-0-25	0	25	10.2
TX-0-50	0	50	10.0
TX-0-100	0	100	10.4
TX-6-25	6	25	8.9
TX-6-50	6	50	9.5
TX-6-100	6	100	9.2
TX-12-25	12	25	8.7
TX-12-50	12	50	8.9
TX-12-100	12	100	8.4

*DS* direct shear test, *TX* triaxial test

sample volume changes was trivial. Table 1 presents the list of performed tests with a brief description of each test.

### 3 Experimental Results and Discussion

Results of the conducted triaxial and direct shear tests are presented in Fig. 2. In the triaxial tests, deviatoric stress increases continuously without any peak stress or asymptote that is in agreement with other researchers reports (Machado et al. 2002; Grisolia et al. 1995; Shariatmadari et al. 2009; Zekkos et al. 2012; Karimpour-Fard et al. 2011; Landva and Clark 1990). However, for all direct shear tests, stress–strain curves tend towards exhibiting a horizontal tangent at large strains.

#### 3.1 Fiber Effects on the Response Shape

Lack of an asymptote in triaxial responses is because of reinforcement role of fibers. Figure 3a shows how

fibers could improve shear strength of MSW. As it could be observed in the triaxial apparatus, the shearing plane passes and cuts through the horizontally oriented plastic fraction with an orientation angle of  $45 + \phi/2$  from a horizontal direction. Thus, the reinforcement action of fibers is mobilized. As a result of reinforcement, deviatoric stress increases continuously and no peak or asymptote is observed in the response.

In direct shear tests, the fiber orientation is almost synchronized with the shear plane (Fig. 3b) and shearing occurs parallel to the fibers. Thus reinforcement action does not mobilize and there will be no improvement in the shearing strength. Therefore, stress reaches an ultimate value at large strains (Fig. 2).

## 4 Hyperbolic Model for MSW

### 4.1 Hyperbolic Model

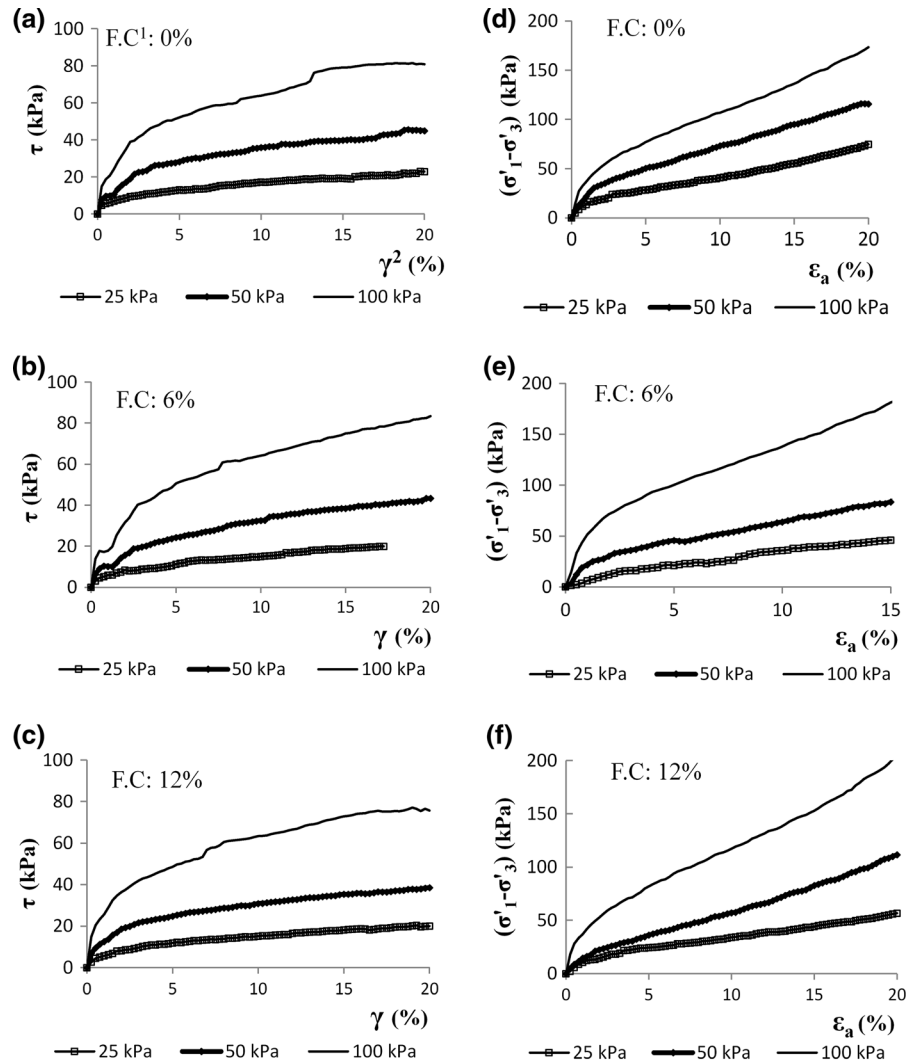
Hyperbolic model is based on typical triaxial test results and provides a framework to represent stress–strain behavior of soils. According to this model, for every strain level, corresponding stress and stiffness are calculated. The initial stiffness is dependent on confining stress. This model has been used widely in geotechnical simulations.

The hyperbolic relationship between stress and strain was first presented by Kondner (1963) and modified by Duncan and Chang (1970) as a six-parameters model. Kondner (1963) introduced an equation to calculate the deviatoric stress as follows:

$$(\sigma'_1 - \sigma'_3) = \frac{\varepsilon_a}{\frac{1}{E_i} + \frac{\varepsilon_a}{(\sigma'_1 - \sigma'_3)_{ult}}} \quad (1)$$

where  $(\sigma'_1 - \sigma'_3)$  = deviatoric stress,  $\varepsilon_a$  = axial strain,  $E_i$  = initial Young modulus and  $(\sigma'_1 - \sigma'_3)_{ult}$  = ultimate deviatoric stress. To get such equation, it is assumed that the stress–strain curve of soil is purely hyperbolic:  $\sigma'_1 - \sigma'_3 = \frac{\varepsilon_a}{a + b\varepsilon_a}$ . Using the latter equation and the tangent Young modulus definition (if  $\sigma'_3$  is constant, then  $E_t = \frac{\partial(\sigma'_1 - \sigma'_3)}{\partial\varepsilon_a}$ ) and applying boundary conditions at strains equal to zero and infinity result in  $a = \frac{1}{E_i}$  and  $b = \frac{1}{(\sigma'_1 - \sigma'_3)_{ult}}$ .

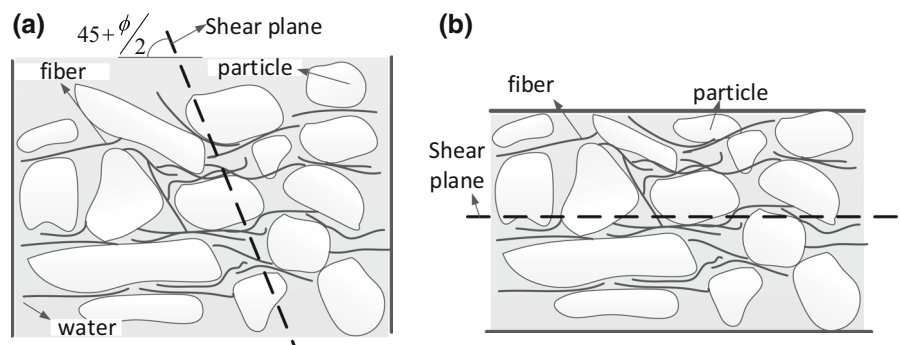
**Fig. 2** Stress–displacement response. **a–c** Results of DS tests and **d–f** results of TX tests



<sup>1</sup>: F.C= fiber content.

<sup>2</sup>:  $\gamma$ = normalized shear displacement ( $\frac{\text{horizontal displacement}}{\text{shear box length}=300 \text{ mm}}$ ).

**Fig. 3** The orientation between shearing plane and fibers. **a** Triaxial device, **b** direct shear apparatus



As indicated in Fig. 4a,  $(\sigma'_1 - \sigma'_3)_{ult} > (\sigma'_1 - \sigma'_3)_f$  and a reduction factor,  $R_f$  is defined as

$$R_f = \frac{(\sigma'_1 - \sigma'_3)_f}{(\sigma'_1 - \sigma'_3)_{ult}} \tag{2}$$

where  $(\sigma'_1 - \sigma'_3)_f$  (or  $\sigma'_{d,f}$ ) is the failure deviatoric stress. Using Mohr–Columb failure criterion,  $(\sigma'_1 - \sigma'_3)_f$  could be represented as

$$(\sigma'_1 - \sigma'_3)_f = \frac{2C' \cos \phi' + 2\sigma'_3 \sin \phi'}{1 - \sin \phi'} \tag{3}$$

Taking the stress dependence of the initial young modulus into account, Janbu (1936) suggested that  $E_i$  varies as:

$$E_i = K P_a \left( \frac{\sigma'_3}{P_a} \right)^n \tag{4}$$

where  $E_i$  = initial young modulus,  $\sigma'_3$  = effective confining stress,  $P_a$  = reference pressure equal to 101.3 kPa, and “K” and “n” are dimensionless parameters to express variations of  $E_i$  vs.  $\sigma'_3$ .

Substituting  $E_i$  and  $(\sigma'_1 - \sigma'_3)_{ult}$  into Eq. (1) gives:

$$(\sigma'_1 - \sigma'_3) = \frac{\epsilon_a}{\frac{1}{K P_a \left( \frac{\sigma'_3}{P_a} \right)^n} + \frac{\epsilon_a R_f (1 - \sin \phi')}{2C' \cos \phi' + 2\sigma'_3 \sin \phi'}} \tag{5}$$

This five-parameters equation could simulate the stress–strain response of many soil types. However calculation of volumetric strain needs Poisson ratio. Figure 4b, c show sequences of calculating  $E_i$ , K, n and  $(\sigma'_1 - \sigma'_3)_{ult}$ .

The hyperbolic model parameters can be obtained easily from the conventional triaxial test. Also it can represent nonlinear, stress-dependent behavior of soils. In addition, the model is simple and has been used widely by researchers and engineers. However, model has several limitations: (1) the model cannot capture dilation or peak stress; (2) this model assumes that  $\sigma'_3 = \sigma'_2$ ; (3) failure could not be modeled realistically since the model uses elastic Hook law whereas material may exhibit plastic behavior; (4) model cannot capture different stress paths. In the case

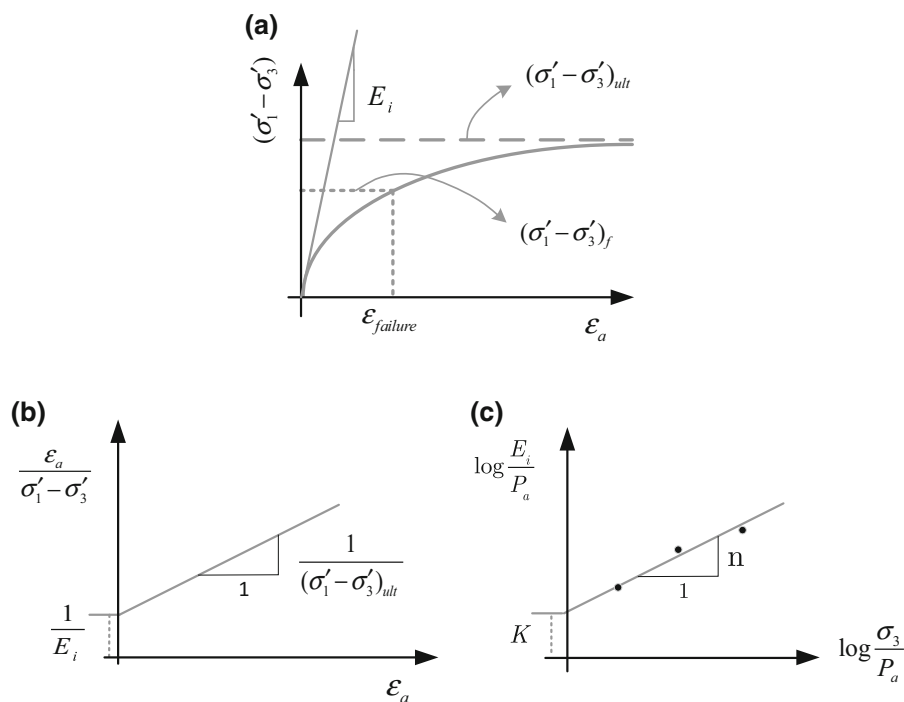


**Fig. 4** a Stress–strain response in triaxial apparatus; hyperbolic model parameters are shown in the graph. b Triaxial test results are plotted on the transformed axes to obtain  $E_i$  and  $(\sigma'_1 - \sigma'_3)_{ult}$ . c calculating ‘K’ and ‘n’ for a set of triaxial tests

of MSW, model may not predict volumetric strain satisfactorily.

### 4.2 Hyperbolic Model for Direct Shear Test Results

In direct shear tests, shear stresses and displacements are distributed within the specimen non-uniformly. Shear stress with normalized horizontal displacement varies hyperbolically in this test and by making some assumptions, the hyperbolic model can be employed for the results. According to this idea, the parameters previously used to develop hyperbolic model for the triaxial test, i.e.  $\sigma_{d,ult}$ ,  $\sigma_{d,f}$ ,  $\sigma_3$ ,  $\epsilon_a$  and  $E_i$ , transform to  $\tau_{ult}$ ,  $\tau_f$ ,  $\sigma_n$ ,  $\gamma$  (normalized horizontal displacement) and  $S_i$  (initial slope of  $\tau - \gamma$  graph). Following the same

steps as what explained before, the hyperbolic equation for the direct shear test is expressed as:

$$\tau = \frac{\gamma}{\frac{1}{KPa_n \left(\frac{\sigma_n}{Pa}\right)^n} + \frac{\gamma R_f}{\sigma_n \cdot \tan\phi + C}} \tag{6}$$

It is worth mentioning that stresses and strains in direct shear box are non-uniform and it is not possible to determine shear strain and shear modulus from this test (ASTM D3080-98 1998). Therefore a new terminology was employed for  $S_i$  and  $\gamma$  which are respectively ‘initial slope of  $\tau - \gamma$  graph’ and ‘normalized horizontal displacement’ instead of shear modulus and shear strain.

### 4.3 Model Validation

As mentioned above, the typical stress–strain response of waste in the triaxial test includes a downward curvature at low strains which continues almost linearly up to a certain strain point (turning point) where it changes to an upward curvature without any peak stress or asymptote. Based on the waste composition and the test conditions, level of turning point and intensity of the upward curvature varies. Generally, as stiffness of waste ingredients increases as well as confining pressure, the upward curvature starts at lower strains and the response shape would not be hyperbolic.

Figure 5 shows the triaxial test results of Zekkos et al. (2012) on wastes with different compositions. The hyperbolic model could not capture the responses at large strains, but it is applicable to lower values of

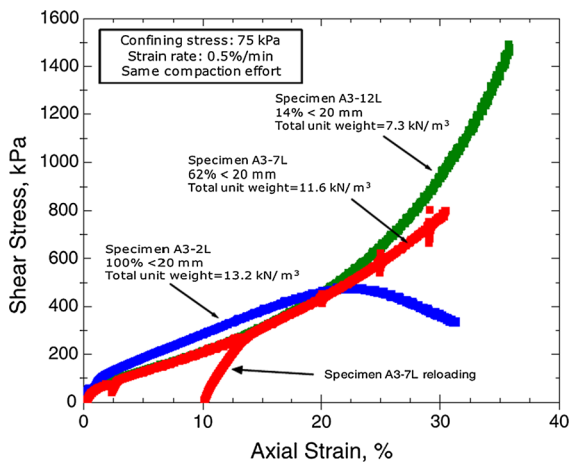


**Fig. 5** Stress–strain response for different composition (Zekkos et al. 2012)

**Table 2** Comparison of hyperbolic model with two MSW models

Model	Model capabilities and features				
	Stress path	Capturing concavity	Considering waste composition	No. of parameters	Required tests to run model
Machado et al. (2002)	Y	Y	Y	14	Triaxial, compression
Machado et al. (2008)	Y	Y	Y	21	Triaxial, compression, *
Babu et al. (2010)	Y	**	N	8	Triaxial, compression
Hyperbolic	N	N	N	6	Triaxial

Y yes, N no

\* Other data is required for material properties, and time dependent parameters

\*\* Under question

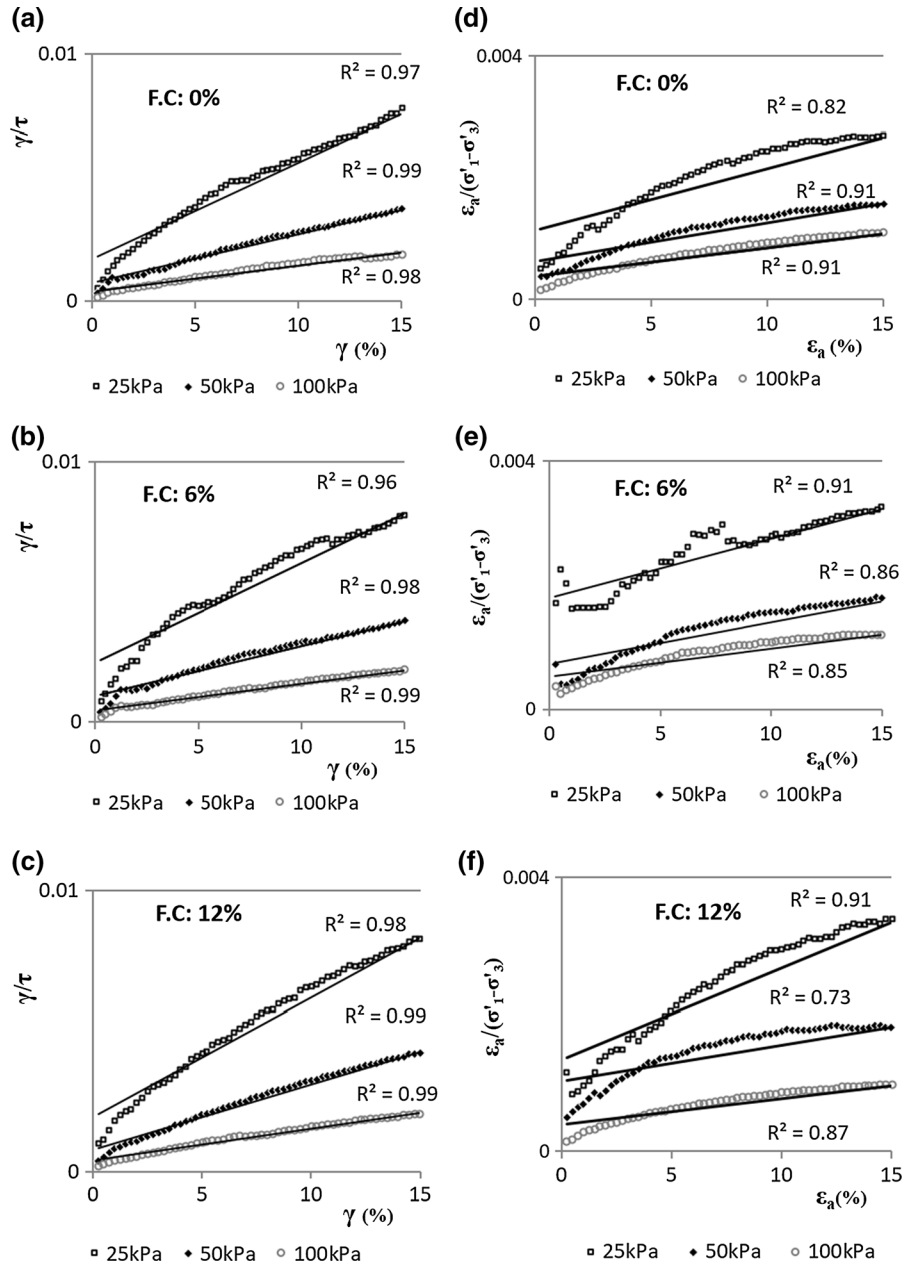


strain. A brief comparison of hyperbolic model with other MSW models is presented in Table 2.

Looking at Eqs. 2, 3 and 5, it would be clear that reproduction of stress–strain graph by hyperbolic model is significantly dependent on selected failure strain. For a satisfactory prediction of MSW response by hyperbolic model, this strain should be lower than the strain at which upward curvature starts because the model cannot capture upward curvature. According to

the previous studies (e.g., Grisolia et al. 1995; Vilar and Carvalho 2002; Machado et al. 2002; Shariatmadari et al. 2009; Zekkos et al. 2012) generally the upward curvature starts at axial strains more than 20% and for strains smaller than 20%, hyperbolic model could be used. This strain is selected by Singh and Fleming (2010) when calculating hyperbolic model parameters. In this study limit strain of 15% was selected as failure strain and shear strength parameters

**Fig. 6** Determination of  $E_i$  and  $(\sigma'_1 - \sigma'_3)_{ult}$  (or  $S_i$  and  $\tau_{ult}$ ): **a–c** for DS tests and **d–f** for TX tests





were calculated based on it. Other model parameters can be obtained following Fig. 4.

Figure 6 shows the stress–strain data plotted on the transformed axes ( $\epsilon_a - \sigma_d/\epsilon_a$  or  $\gamma - \tau/\gamma$ ). For each plot, the inverse of intercept and inverse of slope give values of  $E_i$  (or  $S_i$ ) and  $(\sigma'_1 - \sigma'_3)_{ult}$  (or  $\tau_{ult}$ ), respectively. Next, “K” and “n” are calculated as explained in Fig. 4 for every set of tests. Tables 3 and 4 show hyperbolic model parameters for triaxial and direct shear tests, respectively.

Triaxial and direct shear test responses and their respective hyperbolic graphs are illustrated in Fig. 7. The hyperbolic shape of direct shear test results is clear and has been predictable due to lack of engagement of fibers, as explained before. However in triaxial tests, as a result of fibers effect on mechanical response, precision of model predictions is less.

Parameters of hyperbolic model have been also investigated in literature. Filz et al. (2001) suggested two sets of hyperbolic parameters for stiff and soft MSW. They adopted the hyperbolic model during investigation of landfill failure. Singh and Fleming (2010) also proposed upper and lower bounds values of hyperbolic model parameters ( $K$ ,  $n$ ,  $R_f$ ) for MSW based on analysis of their own triaxial test results and other triaxial test results from different regions of the world. Whenever  $c$ ,  $\phi$  and confining stress are known, the stress–strain upper and lower bounds could be

generated. Table 5 shows the values of proposed parameters.

Figure 8 shows TX-12 response compared with the generated response according to Filz et al. (2001) and Singh and Fleming (2010). Since the  $R_f$  value for soft MSW suggested by Filz et al. (2001) is likely to be wrong, the soft MSW graph has been generated for  $R_f = 0.7$ . According to Fig. 8, in both cases the present results are lower than those proposed by them. This could be attributed to the age of samples (which were fresh) as well as removing or lessening of some objects.

#### 4.4 Fiber Effects on Stiffness

##### 4.4.1 Triaxial Test

Figure 9a shows the  $E_i$  ratio of each confining stress to the  $E_i$  obtained from TX-0-25 test. For each set of triaxial tests, stiffness increases with the confining stress; however, the trends might be different. The stiffness ratio increases linearly with the confining pressure for 0 and 6% of fiber content; however, the rate of increase is higher for the 6% ratio. For 12%, the variation is exponential. There might be a small increase in the stiffness ratio up to 50 kPa of confining pressure, but after this pressure, the stiffness ratio increases significantly.

**Table 3** Hyperbolic model parameters for triaxial test

Sample ID	$\sigma'_3$ (kPa)	$(\sigma'_1 - \sigma'_3)_f$ (kPa)	Estimated (15%)		$R_f$	$R_f^a$	n	K	$\phi$	c (kPa)
			$(\sigma'_1 - \sigma'_3)_{ult}$ (kPa)	$E_i$ (kPa)						
<i>Kahrizak landfill (Tehran, Iran)</i>										
TX-0-25	25	55.4	69.2	1136	0.80	0.8	0.8	33.4	20.2	11.9
TX-0-50	50	95.2	122.9	1943	0.77					
TX-0-100	100	136.3	165.7	3348.3	0.82					
TX-6-25	25	46.0	90.9	586.3	0.51	0.7	1.4	45.0	28.5	0.0
TX-6-50	50	83.8	109.0	1720	0.77					
TX-6-100	100	181.2	216.6	3668	0.84					
TX-12-25	25	44.2	57.6	908	0.77	0.7	0.9	28.7	24.8	2.9
TX-12-50	50	82.7	124.0	1165.4	0.67					
TX-12-100	100	152.9	194.7	3265.7	0.79					

<sup>a</sup> Average reduction factor

**Table 4** Hyperbolic model parameters for direct shear test

Sample ID	$\sigma_n$ (kPa)	$\tau_f$ (kPa)	Estimated (15%)		$R_f$	$R_f^a$	n	K	$\phi$	c (kPa)
			$\tau_{ult}$ (kPa)	$S_i$ (kPa)						
<i>Kahrizak landfill (Tehran, Iran)</i>										
DS-0-25	25	19.4	22.9	706.4	0.85	0.9	1.0	29.4	38.2	0.0
DS-0-50	50	39.7	47.0	1567	0.84					
DS-0-100	100	78.9	88.2	2838	0.89					
DS-6-25	25	18.6	22.9	511.2	0.81	0.8	1.1	24.1	36.9	0.0
DS-6-50	50	38.5	48.0	1101	0.80					
DS-6-100	100	74.1	89.8	2410	0.83					
DS-12-25	25	17.8	21.0	612.7	0.85	0.9	1.1	30.0	35.5	0.0
DS-12-50	50	35.1	39.6	1522	0.89					
DS-12-100	100	72.4	83.0	2855	0.87					

<sup>a</sup> Average reduction factor

**Fig. 7** Stress–strain response and hyperbolic graphs. **a–c** for DS tests, **d–f** for TX tests

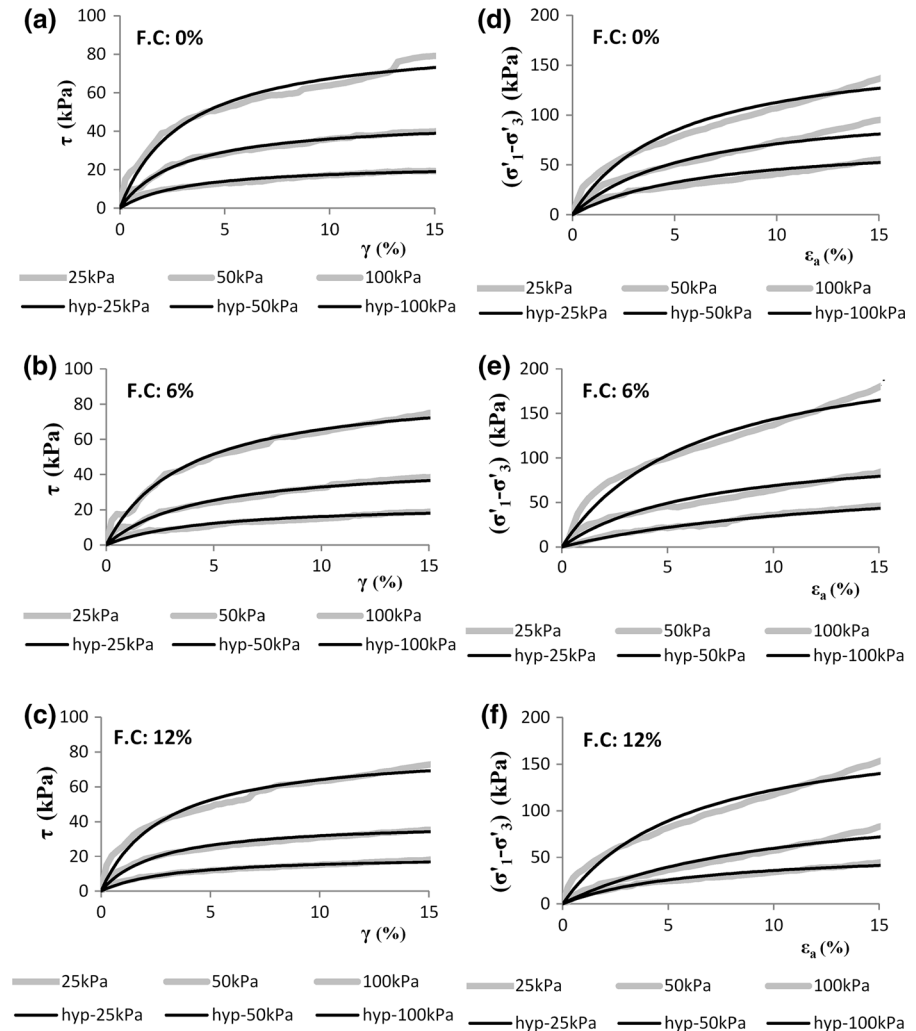


**Table 5** MSW hyperbolic model parameters in the literature

	c (kPa)	$\phi$	K	n	$R_f$
Stiff MSW (Filz et al. 2001)	43	31	90	0.60	0.70
Soft MSW (Filz et al. 2001)	24	30	35	0.40	0.00
Upper-bound stress–strain level (Singh and Fleming 2010)	–	–	58	0.88	0.64
Lower-bound stress–strain level (Singh and Fleming 2010)	–	–	36	0.61	0.82

**Fig. 8** Verification of proposed model with the results of **a** Filz et al. (2001) and **b** Singh and Fleming (2010)

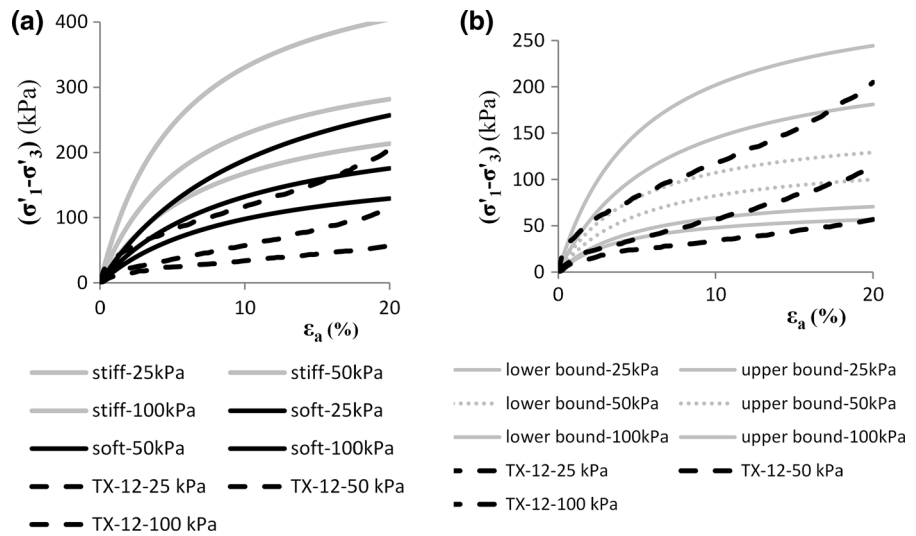
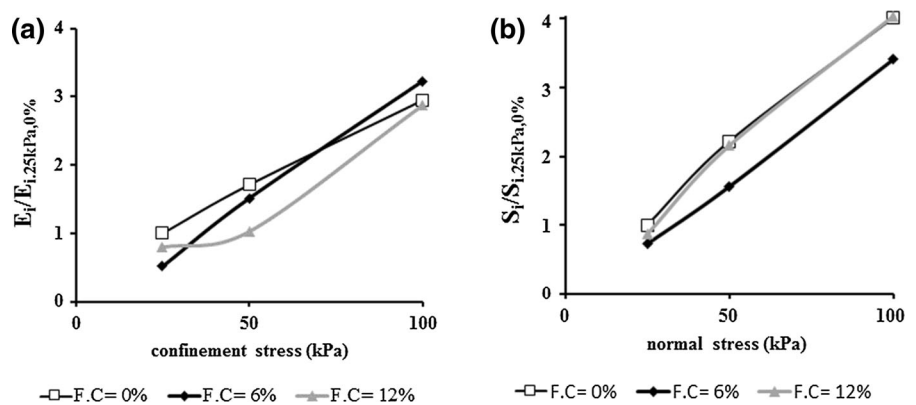


**Fig. 9** Ratio of initial stiffness of each confining (normal) stress to stiffness of TX (or DS)-0-25 kPa sample. **a** Triaxial tests and **b** direct shear tests



In fibrous samples, because fibers behave elastically, there is some rebound in the volume of samples at low levels of confining pressure and therefore less initial stiffness could be achieved. However, this decrease is not obvious at higher confining pressures.

It should also be noted that in the triaxial test, as the shearing goes on, by increasing the mean effective stress, the bondage among the plastic fractions and the surrounding MSW particles increases. Therefore, the reinforcement effect would be mobilized. This has been reported by Machado et al. (2002). Considering

this issue, for confining pressure up to 50 kPa there is a slight change of stiffness in the 12% samples, but in TX-12-100 specimen, high confinement mobilizes the reinforcement action and  $E_i$  increases.

#### 4.4.2 Direct Shear Test

In Fig. 9b the variation of the normalized stiffness in the shearing plane with normal stress for different values of plastic fraction is illustrated.

As observed, the highest value of normalized stiffness occurs at 0% of plastic fraction. By increasing the plastic content to 6 and 12%, the stiffness decreases.

This variations however could be explained as follows:

Based on the findings of Landva and Clark (1990), Zekkos et al. (2010) and Karimpour-Fard et al. (2014), in the direct shear test, by increasing the fiber content, shear strength decreases which is in contradiction with the triaxial test results. Because, in the direct shear test, the plastic fractions tend to align themselves in a horizontal direction during compaction and the shearing progress. Therefore, no engagement between the shearing plane and the plastic fraction could be found in the direct shear test on MSW samples.

This study confirmed applicability of hyperbolic model to capture MSW response. Further investigations including verification of this model by results of field data should be performed to reveal its practical aspects.

## 5 Conclusion

In this study, nine direct shear tests and nine triaxial tests were conducted on MSW samples with different fiber contents to study MSW behavior as the main constituent of a landfill. The results show that in the triaxial tests, fiber addition increases the MSW strength obviously while in the direct shear tests there is a decrease in strength by adding fibers. The dissimilarity is attributed to different shear mechanism of each apparatus.

The second part of this study employed the Duncan and Chung hyperbolic model (1970) to represent the MSW behavior. The model can predict both triaxial and direct shear test results adequately at limited strains. Stiffness variations in triaxial tests are based on the confining pressure. At low confinements, due to the potential rebound tendency of fibers, the contacts between particles decreases, leading to lower stiffness of fibrous samples. But by increasing the confining stress and preventing the rebound of fibers as well as the engagement of reinforcement action of fibers, fibrous samples' stiffness increases. In direct shear tests, fibers generally align horizontally and no engagement could be found between the shearing

plane and plastic fraction. Therefore, there is no increase in the stiffness.

**Acknowledgement** The corresponding author would like to thank Imam Reza for his kindly help. The writers are grateful to Arad Kouh complex waste process and disposal site for their help in collecting samples.

## References

- ASTM D3080-98 (1998) Standard test method for direct shear test of soils under consolidated drained conditions. American Society for Testing and Materials, West Conshohocken. doi:[10.1520/D3080-98](https://doi.org/10.1520/D3080-98)
- ASTM D4767-02 (2002) Test method for consolidated undrained triaxial compression test for cohesive soils. American Society for Testing and Materials. doi:[10.1520/D4767-02](https://doi.org/10.1520/D4767-02)
- Babu SGL, Reddy KR, Chouksey SK (2010) Constitutive model for municipal solid waste incorporating mechanical creep and biodegradation-induced compression. *Waste Manag* 30(1):11–22. doi:[10.1016/j.wasman.2009.09.005](https://doi.org/10.1016/j.wasman.2009.09.005)
- Blight G (2008) Slope failures in municipal solid waste dumps and landfills: a review. *Waste Manage Res* 26(5):448–463. doi:[10.1177/0734242x07087975](https://doi.org/10.1177/0734242x07087975)
- Bray J, Zekkos D, Kavazanjian E, Athanasopoulos G, Riemer M (2009) Shear strength of municipal solid waste. *J Geotech Geoenviron Eng* 135(6):709–722. doi:[10.1061/\(ASCE\)GT.1943-5606.0000063](https://doi.org/10.1061/(ASCE)GT.1943-5606.0000063)
- Carvalho MF (1999) Mechanical behavior of municipal solid waste. University of Sao Paulo, Sao Carlos, SP, Brazil (in Portuguese)
- Duncan JM, Chang CY (1970) Nonlinear analysis of stress and strain in soils. *J Soil Mech Found Div* 96(5):1629–1653
- Filz G, Esterhuizen J, Duncan J (2001) Progressive failure of lined waste impoundments. *J Geotech Geoenviron Eng* 127(10):841–848. doi:[10.1061/\(ASCE\)1090-0241\(2001\)127:10\(841\)](https://doi.org/10.1061/(ASCE)1090-0241(2001)127:10(841))
- Grisolia M, Napoleoni Q, Tancedi G (1995) The use of triaxial test for characterization of MSW. In: Proceedings of Sardinia '95—5th international waste management and landfill symposium, Cagliari, Italy, vol II, pp 761–768
- Janbu N (1936) Soil compressibility as determined by oedometer and triaxial tests. In: European conference on soil mechanics and foundation engineering, Germany, Wiesbaden, pp 19–25
- Jessberger HL, Kockel R (1993) Determination and assessment of the mechanical properties of waste. *Waste disposal by landfill*. Green '93. R.W. Sarsby, pp 313–322
- Karimpour-Fard M, Machado SL, Shariatmadari N, Noorzad A (2011) A laboratory study on the MSW mechanical behavior in triaxial apparatus. *Waste Manag* 31(8):1807–1819
- Karimpour-Fard M, Shariatmadari N, Keramati M, Jafari Kolarijani H (2014) An experimental investigation on the mechanical behavior of MSW. *Int J Civil Eng* 12(4):292–303

- Koerner RM, Soong TY (2000) Leachate in landfills: the stability issues. *Geotext Geomembr* 18(5):293–309
- Kondner RL (1963) Hyperbolic stress–strain response: cohesive soils. *J Soil Mech Found Div* 89(1):115–144
- Landva A, Clark J (1986) Geotechnical testing of waste fill. In: *Proceedings of the 39th Canadian geotechnical conference* Ottawa, Ontario, pp 371–385
- Landva AO, Clark JI (1990) Geotechnics of waste fill. In: Landva A, Knowles D (eds) *Geotechnics of waste fill: theory and practice*. STP No. 1070. ASTM, Philadelphia, PA, pp 86–103
- Machado S, Carvalho M, Vilar O (2002) Constitutive model for municipal solid waste. *J Geotech Geoenviron Eng* 128(11):940–951. doi:[10.1061/\(ASCE\)1090-0241\(2002\)128:11\(940\)](https://doi.org/10.1061/(ASCE)1090-0241(2002)128:11(940))
- Machado SL, Vilar OM, Carvalho MF (2008) Constitutive model for long term municipal solid waste mechanical behavior. *Comput Geotech* 35(5):775–790
- Reddy KR, Kosgi S, Motan ES (1996) Interface shear behavior of landfill composite liner systems: a finite element analysis. *Geosynth Int* 3(2):247–275
- Shariatmadari N, Machado SL, Noorzad A, Karimpour-Fard M (2009) Municipal solid waste effective stress analysis. *Waste Manag* 29(12):2918–2930
- Shariatmadari N, Sadeghpour AH, Razaghian F (2014) Effects of aging on shear strength behavior of municipal solid waste. *Int J Civil Eng* 12(3 and B):226–237
- Singh MK, Fleming IR (2010) Application of a hyperbolic model to municipal solid waste. *Geotechnique* 61(7):533–547. doi:[10.1680/geot.8.P.051](https://doi.org/10.1680/geot.8.P.051)
- Vilar OM, Carvalho MF (2002) Shear strength properties of municipal solid waste. In: *Proceeding of the fourth international congress on environmental geotechnics, Brazil*, pp 59–64
- Vilar OM, Carvalho MF (2004) Mechanical properties of municipal solid waste. *J Test Eval* 32(6):1–12
- Wood DM (2003) *Geotechnical modelling*, vol 1. CRC Press, Boca Raton
- Zekkos D, Athanasopoulos GA, Bray JD, Grizi A, Theodoratos A (2010) Large-scale direct shear testing of municipal solid waste. *Waste Manag* 30(8–9):1544–1555
- Zekkos D, Bray JD, Riemer MF (2012) Drained response of municipal solid waste in large-scale triaxial shear testing. *Waste Manag* 32(10):1873–1885